ALLEVIATION OF ATMOSPHERIC FLOW DISTURBANCE EFFECTS ON AIRCRAFT RESPONSE

Klaus-Uwe Hahn, Carsten Schwarz
DLR – German Aerospace Center, Institute of Flight Systems
Lilienthalplatz 7, 38108 Braunschweig, Germany

Keywords: *Wake Vortex, Gusts, Aircraft Response, Disturbance Measurement, Control*

Abstract

Since the air is the element of flying, air motion is an essential parameter in aeronautics. This paper gives an overview of the results of offline simulations, full flight simulator studies and results from in-flight simulation experiments to investigate the alleviation of atmospheric flow disturbance effects on aircraft response. The studies are part of the DLR project "Weather and Aviation" aiming at the improvement of flight operation and safety in adverse weather conditions.

Gusts and turbulence strongly affect the passenger comfort and the safety of aircraft. Another important air mass motion adversely affecting aircraft operation is wake vortex. This well known hazardous flow field is produced by aircraft themselves. Active control technology can be applied to alleviate these flow disturbance effects on aircraft motion in case of an encounter.

DLR is developing the Integrated Ride and Loads Improvement System (IRLIS) to cope with the phenomena mentioned above. It can be shown that the aircraft response encountering natural and aircraft-induced (wake vortex) turbulence can be improved significantly by a feed-forward controller. Based on a forward-looking sensor, the controller generates aero-dynamic surface deflections to counter the vertical accelerations generated by gusts as well as the roll response induced by lift variations along the wing span. For this investigation it is assumed that a LIDAR sensor is able to provide the necessary flow field information ahead of the a/c. In addition to the standard control surfaces (elevator, aileron and rudder) the a/c is supposed to be equipped with special flaps for independent direct lift control. Simulation results show a clear tendency that IRLIS can significantly improve the situation in adverse atmospheric flow fields.

List of Symbols, Abbreviations and Acronyms

H	height
K	gain
L	lift
M	moment
f	frequency
q	pitch rate
r	yaw rate
t	time
v	lateral velocity component
V	airspeed (no index), velocity
w	vertical velocity component
x	longitudinal x coordinate
α	angle of attack
β	angle of sideslip
δ	control surface deflection
ε	*downwash angle*
χ	flight path azimuth
γ	flight path angle
η	elevator deflection
σ	standard deviation
τ	time delay
ξ	aileron deflection
ζ	rudder deflection
Δ	difference
Φ	bank angle
Θ	pitch angle
Ψ	heading
DLC	direct lift control
F	follower (WV encountering a/c)

g	geodetic (refers to earth fixed coordinates)
wing-HTP	from wing to HTP
K	kinetic (refers to flight path)
L	leader (WV generating a/c)
pos	Position
AoA	angle of attack
AoA-wing	from AoA sensor to wing
AoS	angle of sideslip
W	wind
WV	wake vortex
WVL	wake vortex line
1, 2, …	index
•	denotes a time derivative
→	denotes a vector
*	denotes a normalized parameter

a/c	aircraft
ADS-B	Automatic Dependent Surveillance-Broadcast
AP	auto pilot
AWIATOR	Aircraft Wing with Advanced Technology Operation
ATTAS	Advanced Technologies Testing Aircraft System
DLR	German Aerospace Center
DLC	direct lift control
FF	feed-forward
FbW	Fly-By-Wire
GCS	Gust Computation System
GLAS	Gust Load Alleviation System
HTP	horizontal tail plane
IMC	instrumental meteorological conditions
IFS	in-flight simulation
IRLIS	Integrated Ride and Loads Improvement System
IRS	Intertial Reference System
LARS	Load and Ride Smoothing System
LIDAR	Light Detection and Ranging
MTOW	maximum take-off weight
MLW	maximum landing weight
RWY	runway
THR	threshold

1 Introduction

Atmospheric flow disturbances adversely affect aircraft motion and flight safety. This applies to natural gusts and turbulence and to aircraft self-induced wake vortices if encountered by trailing aircraft. Although the term “wake vortex turbulence” is often used, the aircraft response to wake vortex encounters can be very different from its behavior in homogeneous natural turbulence.

The idea of improving the aircraft response and the corresponding loads in gusts and turbulence is not new. There were some promising attempts in the past to use active control technology to counteract atmospheric disturbances [1,2,3,4]. A very successful concept was flight tested during the 1990s. This Load Alleviation and Ride Smoothing System (LARS) was demonstrated on DLR’s flying testbed VFW614/ATTAS (Advanced Technologies Testing System) [5]. Based on the LARS concept even an approach for the alleviation of horizontal accelerations was successfully flight tested [6]. The LARS concept was also applied in the frame of the European AWIATOR project. In addition a dynamic feed-forward controller for the alleviation of the wing root bending moment was developed [7]. A sophisticated design for elastic modes control is presented in [8].

DLR can also show a similar experience and long term history for its activities in the area of the wake vortex phenomenon [9, 10]. Starting in 1999 DLR has re-established and increased its efforts on this subject, setting up two consecutive projects named “*Wirbelschleppe I”* and *“Wirbelschleppe II”* (*Wirbelschleppe* means *wake vortex*). They were dedicated to the full spectrum of the wake vortex phenomenon. Besides the investigations to increase and improve the knowledge and understanding of the wake vortex phenomenon itself, passive and active measures to diminish their creation and a controller concept were developed. By means of simulator studies and real flight tests (in-flight simulations) the potential of the concept was demonstrated [11,12].

The effect of air mass motion on aircraft can be very varied. The scale of the flow fluctuation related to aircraft dimensions, respectively wing span and wing depth, plays an important role for the respective impact. While low frequency flow fluctuations have a significant impact on the energy state of the

aircraft [13-15] the higher frequencies will produce unwanted accelerations of the aircraft. This paper will concentrate on the latter effects.

1.1 The new DLR Project "Weather and Aviation"

DLR has started in 2008 a new comprehensive project named "*Wetter und Fliegen*" (*Weather and Aviation*). This project was established to transfer the accumulated experience into the practice of actual flight operation.

The project considers the most important aspects of atmospheric disturbances like natural gusts and turbulence, aircraft-induced wake vortices and thunderstorms. To minimize the impact of adverse weather conditions a combination of measures for air traffic management, strategical and tactical avoidance maneuvering, and active control methodologies will be developed and investigated. This paper will focus on the part of the project devoted to controlled flight in adverse atmospheric flow fields. The main goal of the investigations is the unification of active control concepts for the improvement of aircraft response in gusts and turbulence, for wake vortex encounters, and in low frequency wind shear. In the following the first results of actively controlled flight in adverse atmospheric flow fields will be presented.

1.2 Principle of Disturbance Compensation

Considering the experience from the design of control systems for gust load alleviation, wake vortex mitigation, and wind shear compensation [3-7,9-15] the authors are convinced that atmospheric disturbances can be treated best using feed-forward (FF) control. The advantage of such a disturbance compensation concept is that the counteractions are initiated before the aircraft response sets in. Furthermore this approach has the advantage of leaving the original aircraft dynamics and handling qualities unchanged since such a control system is only active if an external disturbance is detected.

For the application of the FF concept the flow disturbance acting on the aircraft has to be known. The vector of the flow disturbances $\vec{V}_W$ can be calculated by

$$\vec{V}_W = \vec{V}_K - \vec{V}\,. \qquad (1)$$

The inertial speed vector $\vec{V}_K$ is available from the inertial reference system (IRS). The airspeed vector $\vec{V}$ is measured by flow probes.

Knowing the aerodynamics of the respective aircraft the flow disturbance-induced aerodynamic force and moment variations can be calculated. Depending on the available (standard and potentially special) control surfaces the necessary commands for best countermeasures can be computed.

Assuming complete aerodynamic force and moment control the FF controller will fully compensate for the flow disturbances within the range of the actuator limits. Real aircraft normally are lacking this ideal control capability and provide moment control using elevator, aileron, and rudder, the common primary controls of aircraft. To account for real world effects, and to deal with parameter uncertainties an additional feedback controller can be added to improve the system [11].

2 Normal Load Alleviation

2.1 Effects of Gusts and Turbulence on Aircraft

In the following only the motion of the rigid aircraft without any elastic effects will be considered. For the creation of perceptible accelerations of the aircraft the flow disturbances have to act on the whole wing. Horizontal gusts and turbulence affect the aerodynamic forces mainly due to dynamic pressure variations. Vertical atmospheric currents directly change the angle of attack. The latter effect is the more significant one concerning load factor variations. Wake vortex encounters which are roughly perpendicular to the vortex axis create rapid angle of attack variations all over the wing like discrete strong gusts (Fig. 1). The effects of vertical gusts do not only affect adversely the passenger comfort but also produce significant wing loads.

2.2 Feed-Forward Gust Alleviation

To avoid unwanted aircraft motions the aerodynamic forces have to be maintained constant. The rapid changes in lift induced by gusts and turbulence cannot be compensated by a respective correction of angle of attack using the elevator. Besides the relatively slow pitch dynamics (compared to gust-induced angle of attack variations) the adverse effect of aircraft pitching on passengers, especially the ones sitting in the front and rear part of the fuselage, prohibits such a concept. The best suited concept for rapid lift control is provided by special fast flaps allowing camber variations. This can be achieved by direct lift control (DLC) flaps mounted at the landing flap's trailing edge (Fig. 2). Such devices are used for the presented feed-forward gust alleviation system. For the calculation of the required DLC-flaps deflection a flow disturbance determination is required.

2.2.1 Disturbance Measurement

The effect of vertical gust velocity w_{Wg} on angle of attack can be expressed by the wind angle of attack α_W [7]

$$\alpha_W \approx -\arcsin\left(\frac{w_{Wg}}{V}\right) \qquad (2)$$

Since neither w_{Wg} nor α_W can be measured directly, α_W has to be computed by [16]

$$\alpha_W \approx \cos(\Phi)\cdot\left\{\arcsin\left(\frac{\dot{H}}{V}\right) - \Theta + \left[\alpha + \frac{q\cdot x_{AoA}}{V}\right]\cdot\cos(\Phi) + \left[\beta - \frac{r\cdot x_{AoB}}{V}\right]\cdot\sin(\Phi)\right\} \qquad (3)$$

where Φ is the roll angle, $\dot{H}$ is the inertial vertical speed of the aircraft, V is the true airspeed, Θ is the pitch angle, α is the angle of attack (AoA), q is the pitch rate, x_{AoA} is the distance between the center of gravity and the AoA-sensor, β is the angle of sideslip (AoS), r is the yaw rate, and x_{AoS} is the distance between the centre of gravity and the AoS-sensor. Eq. (3) can be applied if the position of the measurement is close to the body-fixed longitudinal axis of the a/c.

The consideration of the angle of sideslip in the presence of bank angles (called β-compensation) is very important if an angle of sideslip occurs. Eq. (3) is generally applicable to maneuvering aircraft, during turns as well as for maneuvers with high dynamics. Fig. 3 gives the results of a horizontal turn with a bank angle of $\Phi \approx 45°$ through a gust with a 1-cos-shape and a maximum downwind amplitude of $w_{Wg} = 5m/s$. The importance of the correct processing of AoA and AoS signals is evident. The α_W calculation based only on the AoA signal (blue line) will result in significant deviations compared with the correct time history (red line) which is completely hidden by the green curve computed by Eq. (3) [7].

Based on the assumption (see above) that the extension of the vertical gust is large compared to the a/c dimensions, a single spot measurement of the flow field is adequate for the disturbance determination. To compensate for system delays [5], e.g. computation delays and actuator dynamics, the airflow has to be measured in front of the aircraft before it hits the wing, which is the main lift producing surface. Such an ahead-measurement of the airspeed vector (amplitude V, and direction angles α and β) is possible e.g. with a 5-hole probe mounted at the aircraft's nose or mounted on a boom reaching into the airflow in front of the a/c. But the best forward measurement is expected to be provided by the use of LIDAR technology [24-26]. It is expected that within a few years this technology will have the maturity to provide the relevant airspeed information with the required precision [27].

2.2.2 Feed-Forward Controller

α_W being a measure for the disturbance can be used to calculate the required deflections of the control surfaces to counteract the disturbance. These actions have to be synchronized as illustrated in Fig. 4. The wind angle of attack computed by Eq. (3) is calculated at the position of the flow probe and is assumed to be time independent when it passes the a/c. To compensate the gust-induced lift the DLC-flaps mounted at the wing have to be deflected (gain K1) when the computed wind disturbance reaches the wing position. Therefore the time shift between the measured wind disturbance at the position of the flow probe (ahead of the

wing) and its arrival at the wing has to be taken into account. The delay to be considered is $\tau_{AoA-wing}$. When the gust reaches the wing it not only affects the lift but also the pitch moment equilibrium of the a/c which needs an immediate compensation by the elevator (gain K22). The DLC-flap deflections themselves also produce pitching moments which again have to be compensated by the elevator (gain K21). When the changed downwash of the wing (gain K23) and also the gust itself (gain K24) reach the elevator position, additional elevator deflections are required to avoid pitching of the a/c.

2.2.3 Simulation and Flight Test Results

The feed-forward concept sketched in Fig. 4 was realized and demonstrated in the LARS project [4,5,6]. It was successfully flight tested using ATTAS. For the LARS flight tests a flight-log mounted at a noseboom was used for airspeed vector measurement. LARS achieved a reduction of vertical acceleration in homogeneous turbulence up to more than 10dB within the frequency range of 0.2Hz < f < 2Hz as illustrated in Fig. 5. Comparing the power spectral densities of the vertical load factor with and without the loads alleviation system the improvement is evident.

The same approach was used for the rigid body part of the Gust Load Alleviation System (GLAS) developed within the European AWIATOR project. For the GLAS concept a dynamic feed-forward path controlling the wing bending oscillation was added. GLAS was designed by means of multi-objective optimization. Comprehensive simulations show significant reductions of vertical accelerations and wing root bending moments. Furthermore it was demonstrated that for large transport type a/c at lower airspeed (landing approach) conventional α- and β- and dynamic pressure probes are adequate to serve as airspeed vector sensors. For higher speeds (cruise flight) the usage of a LIDAR is needed to measure the airspeed vector providing sufficient time for the compensation of computation time and system delays [7].

3 Wake Vortex Induced Moment Compensation

3.1 Effect of Wake Vortex on Aircraft

The effects of wake vortices on aircraft are widely varying. Encounters perpendicular to the vortex axis will lead to substantial vertical load factor variations by inducing rapid and large angle of attack variations all over the whole wing comparable to gusts discussed in the sections above. Another situation is present if the flight path of the encountering aircraft runs parallel to the vortex axis. Then the vortex flow will induce varying angles of attack along the wing span producing strong rolling moments which can create significant roll rates resulting in large bank angles. Between these two cases a broad variety of encounter situations exists. In any case the wake vortex produces an adverse effect on aircraft motion. The following chapter will focus on parallel like encounters.

3.2 Aerodynamic Interaction Model (AIM)

The effect of disturbance variation along the wingspan on aircraft is computed following the strip model approach [17]. This model calculates the forces and moments from the local wind angle of attack α_W computed at different sections, so called strips, along the wing and along the horizontal stabilizer as well as along the vertical tail.

This method was deemed feasible in [18], verified against wind tunnel tests in [19] and validated by parameter identification applied to flight test data in [20,21]. The results indicate that the model is suitable to represent wake vortex encounter situations with a potential for improvement for the lateral and the yaw motion.

For transport-type aircraft with a swept wing at least 16 strips are required for the wing, 8 strips should be chosen for the horizontal stabilizer and 4 strips are needed for the vertical fin. An increased number of strips will provide only a minor improvement of the model output.

3.3 Wake Vortex Controller

The wake vortex controller has to be understood as a controller not controlling the wake vortex itself but its effect on aircraft response. The aircraft reaction during wake vortex penetration can be improved by a pilot assistance system based again on a feed-forward control concept. For this wake vortex controller it is necessary to measure the airflow ahead of the aircraft over the whole wing span.

3.3.1 Disturbance Measurement

The required forward-looking measurement of the airspeed vector in wing span direction can be achieved with modern LIDAR technology [24-27]. The LIDAR technique offers the possibility to have a multitude of measurement spots in front of the aircraft where the airspeed vector is determined. Thus, the LIDAR provides sufficient information to compute the wind angle of attack distribution along the wing.

It should be noted that instead of using direct multi-point measurements of the airspeed vector along the wing with a succeeding calculation of the corresponding α_W distribution other approaches are feasible. DLR is working on a concept based on the usage of some characteristic parameters (vortex circulation, vortex position, core radius, and distance of the vortex pair) extracted from LIDAR measurements. This concept allows the estimation of the wake vortex flow field using a mathematical model of the flow phenomenon by means of on-line parameter identification [20,21]. The concept can be improved by data transmitted (e.g. via ADS-B) by the vortex generating a/c (mass, airspeed, configuration, trajectory, and wind along the trajectory). But this concept is still subject of ongoing investigations.

3.3.2 Controller Concept

The feed-forward concept (Fig. 6) reacts based on the measured wake vortex velocities, which are fed into the aerodynamic interaction model described above [11]. The calculated moments are then used with an inverted aerodynamic model of control efficiency to compute appropriate command inputs to aileron, rudder, and elevator for the alleviation of the aircraft response due to the vortex.

3.3.3 Simulation and Flight Test Results

The feed-forward concept of chapter 3.3.2 is analysed using offline simulations of a landing approach situation. Due to the absence of a pilot and in order to maintain the required flight path a regular AP (based on a model following controller concept) is applied [11]. Simulation runs have been performed to investigate the potential of the wake vortex controller.

In Fig. 7 the encounter scenario is sketched. The simulated encountering aircraft is the ATTAS aircraft (ICAO class 'medium', MTOW = 20t). The vortex generating aircraft is another category 'medium' aircraft (MTOW = 94t) with an actual landing weight of MLW = 80t producing a wake vortex which has an age of $t = 90$ s. The encounter angle in the horizontal plane between flight path and vortex lines is $\Delta\psi_{WVL} \approx 4°$. This situation can be considered to be a parallel vortex encounter. The sensors are modelled ideally so that the exact disturbance is known to the controller.

Fig. 8 shows an example flight crossing closely above a wake vortex flow field. The vortex lines are assumed to be $\Delta H \approx 5$m below the nominal approach path to produce a situation at the control limit of the a/c where roughly 100% of the available maximum roll control power is needed. The blue curves show the results with just the AP. The red curves give the results with a combination of AP and wake vortex controller. The side view and the helicopter view show the flight path with the wake vortex encounter scenario. The reference flight path (green dashed line) is inclined with 3° representing an approach situation. The wake vortex (black dashed line) has the same inclination as the nominal flight path (see side view) and an encounter angle of $\Delta\psi_{WVL} \approx 4°$ (see helicopter view). In Fig. 9 the time histories of flight parameters and control commands normalized with the maximum possible amplitudes are illustrated.

The AP is able to cope with the wake vortex to a certain degree showing large bank angle variations and noticeable vertical and lateral flight path excursions. The maximum roll control power is exceeded ($\xi^* > 1$) for a short period. The wake vortex controller assists the AP system and improves the situation

significantly, especially with respect to bank angle deviations which are considerably reduced.

This principle of the wake vortex control system has also been tested with pilots-in-the-loop in simulators as well as with in-flight simulations using DLR's FbW test aircraft ATTAS. In-flight simulation (IFS) is to be understood as a simulation during the real flight. The experimental pilot is using his real controls. These inputs are fed into the onboard computer system stimulating the simulated a/c which reacts on the pilots inputs and on the effects coming from the simulated virtual wake vortex flow. The resulting simulated a/c response is fed into a model following control system which calculates the control surface deflections of the real host a/c (ATTAS) to make it behave like the simulated a/c encountering a wake vortex situation [28]. IFS can be regarded to be the most realistic simulation tool since it takes place within the real world environment of flying.

For the subjective assessment of the wake vortex encounters a dedicated pilot rating scale with four categories (aircraft control, demands on the pilot, aircraft excursions from flight state and path and overall hazard) and four levels has been developed [22] to be used in piloted investigations. The best rating (encounter situation not an issue) is "1" the worst rating is "4" describing an unacceptable situation which the pilot would have avoided. The results in Fig. 10 come from in-flight simulation flight tests. Altogether 9 approaches were conducted in fine weather, 7 approaches were executed in IMC and 4 in light turbulence. Although they present only 20 approaches (12 approaches with assistance system, 8 without) the trend can clearly be seen. The results show a clear tendency that the wake vortex controller improves the situation, resulting in better pilot ratings.

3.4 Measurement Strategies

The wake vortex controller strongly depends on the forward-looking multi-point disturbance measurement provided by the LIDAR. Different measurement strategies for the LIDAR were investigated with offline simulations [23]. Various concepts of orientation of the forward looking LIDAR beam (airframe fixed or flight path fixed) and dimension of the data field (scanning along a line in front of the wing or scanning a plane ahead of the a/c perpendicular to the flight direction) in combination with data processing (with or without interpolation in the data field to account for the a/c motion in the period between the moment when the forward looking measurement was executed and the time when the a/c reaches the respective position ahead) have been developed (see Table 1).

Table 1: Forward-looking measurement strategies

concept	measurement		data processing
	direction of forward looking LIDAR beam	dimension of LIDAR scanning field	interpolationw ith ref. to actual a/c position
1	Airframe fixed	1D (line)	no
2	air path fixed	1D (line)	no
3	air path fixed	1D (line)	wing span direction
4	air path fixed	2D (plane)	wing span and vertical direction

For concept 1 the LIDAR beam is staring airframe-fixed scanning along a horizontal line in wing span direction ahead of the a/c. It cannot be guaranteed that the a/c will really pass the location where the measurements took place. Here it is simply assumed that the airflow will arrive delayed at the aircraft's wing. To enhance the quality of the measurement the LIDAR orientation is chosen to scan a horizontal line in wing span direction ahead of the a/c in the direction of the current air path (concept 2). Here the assumption is made that the a/c will reach the location of the LIDAR measurement following its air path direction at the moment when the measurement was executed. Concept 3 is identical with concept 2 but the actual wing position is interpolated within the measurement points of the scanned horizontal line in front of the a/c. Concept 4 is identical with concept 3 but it considers in addition to the lateral a/c displacement also vertical shifts of the a/c. To account for lateral and vertical a/c displacements a two dimensional pattern is

scanned in front of the wing. Then when the a/c reaches the location where the forward looking measurement was executed the actual wing position is interpolated in this two dimensional measurement plane (Fig. 11).

A comparison between the four measurement concepts is shown in Fig. 12. This figure comes from offline landing approach simulations using AP in combination with the wake vortex controller using the measurement strategies listed in Table 1. Here the absolute value of the maximum bank angle which occurred during controlled parallel like wake vortex penetrations is plotted against the measurement distance. It can simply be stated that the smaller the maximum bank angle the better the measurement strategy.

It is obvious that the flow field has to be scanned in air path direction. The best results were achieved with the two-dimensional measurement and interpolation of concept 4. But for short look-ahead distances below 150m (just to compensate for system delays) an air path fixed measurement seems to be sufficient. Further investigations of the parallel like encounter during landing approach yielded a required sampling rate of $f > 3$Hz. The lateral grid size for the measurements should be less than 10% of the encounter aircraft's wing span. The lateral size of the measurement plane should be at least ±1.25 times the wing span and (for concept 4) vertically at least ±50% of the span.

4 Integrated Ride and Loads Improvement System (IRLIS)

4.1 Controller Concept

The gust load alleviation concept presented in chapter 2 was based on a single spot disturbance information (α_W). Applying the measurement strategies of chapter 3.4, detailed local information of small scale flow variations along the wing can be considered. The AIM then provides the forces and moments induced by these flow disturbances. The controller concept presented in chapter 3.3.2 uses only the conventional control surfaces aileron, rudder, and elevator. For an aircraft equipped with DLC-flaps the disturbance induced lift variation can also be directly controlled. This extended controller concept is sketched in Fig. 13. This concept is the first stage of the Integrated Ride and Loads Improvement System (IRLIS) to be completed in the future.

Applying the IRLIS control concept again in combination with an AP for the landing approach in a simulated wake vortex encounter gives the following results.

4.2 Simulation Results

A nearly parallel encounter (encounter angle: $\Delta\psi_{WVL} \approx 4°$, same conditions as applied for Fig. 8 and Fig. 9) is illustrated in Fig. 14 and Fig. 15. The aircraft response is similar to what was achieved using the combination of AP plus wake vortex controller. The glide path tracking in lateral direction shows no substantial difference due to the DLC-operation and vertical path deviation is only slightly better, but the system alleviates the normal accelerations of the aircraft within its physical limits (max. deflection $|\delta_{DLC}|_{max} < 20°$) as expected.

Fig. 16 and Fig. 17 show a wake vortex encounter with an encounter angle of $\Delta\psi_{WVL} \approx 30°$. For such an encounter angle the situation can no longer be considered to be a parallel like encounter. The vortices induced only very small rolling moments. This case is comparable to a discrete gust producing normal load factors and only little bank. It can be seen that IRLIS performs very well and can be assumed to operate in the complete range of gusts and wake turbulence. The normal load factor is significantly reduced. The roll response is negligible.

5 Summary

State of the art fly-by-wire technology of modern aircraft allows in principle the implementation of additional control algorithms. The progress of LIDAR technology during recent years creates high expectations for having an operational on-board system in the near future providing the performance necessary for

flow field measurements at short distances (less than 100m) ahead of the aircraft. The use of such a scanning LIDAR will provide multi-point flow field information, which offers a powerful option for flow disturbance compensation.

Based on a long history of activities in the area of flying in disturbed atmosphere DLR is going to develop an Integrated Ride and Loads Improvement System IRLIS. The paper presents the first results towards a fully integrated system to counteract the complete spectrum of atmospheric flow disturbances by using all available standard and even new and special control devices.

In a first step the feasibility of an integrated controller design for alleviating normal loads due to gusts and turbulence as well as wake vortex induced rolling motions was investigated. From the experience of the gust load alleviation system LARS and a wake vortex controller flight tested in the past on DLR's flying testbed ATTAS the novel IRLIS concept was designed. It uses a feed-forward design, which has the advantage of leaving the original aircraft dynamics and handling qualities unchanged, and flow field information from a LIDAR sensor to predict the induced forces and moments. This can be done by means of an aerodynamic interaction model (so called strip model). Knowing precisely the aerodynamic effectiveness of the control devices of the aircraft, the required control surface deflections to counteract the disturbances can be calculated. Using offline simulations the capability of the concept is demonstrated. It is shown that significant improvements of roll response and normal loads can be achieved.

The IRLIS system at its present status (described in this paper) will be flight tested in 2009 using in-flight simulation. In a follow-on step IRLIS will be extended by the use of spoilers and continuous flap setting to improve its alleviation performance. Finally a thrust controller will be developed and introduced to provide the capability of coping with low frequency atmospheric motions like wind shear.

References

[1] Schänzer G. Direct Lift Control for Flight Path Control and Gust Alleviation. *AGARD-CP-240*, 1977.

[2] O'Connel R F. Design, Development and Implementation of a Control System for Load Alleviation for a Commercial Transport Airplane. *AGARD-R-683*, Porz-Wahn, 1979.

[3] Böhret H, Krag B and Skudridakis J. OLGA – An Open-Loop Gust Alleviation System. *AGARD-CP-384*, 1985.

[4] König R, Hahn K-U, and Winter J. Advanced Gust Management Systems - Lessons Learned and Perspectives. *AGARD-CP-560*, 1994.

[5] König R and Hahn K-U. Load Alleviation and Ride Smoothing Investigations Using ATTAS. *17th Congress of the International Council of the Aeronautical Sciences*, Stockholm, Sweden, pp 1379-1393, 1990.

[6] Hahn K-U and König R. ATTAS Flight Test and Simulation Results of the Advanced Gust Management System LARS. *AIAA Atmospheric Flight Mechanics Conference*, Hilton Head Island, SC, pp 58-70, 1992.

[7] Hecker S and Hahn K-U. Advanced Gust Load Alleviation System for Large Flexible Aircraft. *Deutscher Luft- und Raumfahrtkongress 2007, First CEAS European Air and Space Conference*, CEAS 2007-110, Berlin, Germany, 2007.

[8] Enzinger M. *A Modal Control Approach Based on a Minimum-Order Dynamic Feedback*. Dissertation FernUniversität in Hagen, Hagen, Germany, 2007.

[9] Weber O. *Detailliertes Meß- und Auswerteprogramm zur Ermittlung der Wirbelschleppenwanderung und Wirbelstärke zwischen den Gleitpfaden 25R und 25L des Verkehrflughafens Frankfurt/Main*. DFVLR IB 111-82/13, Braunschweig, Germany, 1982.

[10] König R. Aircraft Response and Pilot Behaviour During a Wake Vortex Encounter Perpendicular to the Vortex Axis. *AGARD-CP-470*, Gol, Norway, pp 17/1-17/18, 1989.

[11] Hahn K-U. Coping with Wake Vortex. *23rd Congress of the International Council of the Aeronautical Sciences,* Toronto, Canada, 2002.

[12] Schwarz C and Hahn K-U. Automated Pilot Assistance for Wake Vortex Encounter. *Deutscher Luft- und Raumfahrtkongress 2007, First CEAS European Air and Space Conference*, CEAS 2007-006, Berlin, Germany, 2007.

[13] Hahn K-U. Takeoff and Landing in a Downburst. *Journal of Aircraft*, Vol. 24, No. 8, New York, 1987.

[14] Hahn K-U. Effect of Wind Shear on Flight Safety. *Progress in Aerospace Sciences*, Vol. 26, pp 225-259, 1989.

[15] König R. *Beiträge zur Erhöhung der Flugsicherheit in Windscherungen*. Dissertation Technische Universität Braunschweig, Braunschweig, Germany, 1987.

[16] Hahn K-U. *Verfahren zur Reduzierung der Turbulenz- und Böeneinflüsse auf das Flugverhalten von Luftfahrzeugen und Steuerungseinrichtung hierfür. Bundesrepublik Deutschland*, Patent Nr. 102005020660, München, Germany, 2007.

[17] Escande B. *FORTRAN code of strip method for implementation into simulators - Documentation (Version 2)*, SWAKE-D-212_1, 2001.

[18] Barrows T M. Simplified Methods of Predicting Aircraft Rolling Moments due to Vortex Encounters, AIAA 76-61, *AIAA 14th Aerospace Sciences Meeting,* Washington, DC, Jan. 1976.

[19] Bruin A. de, *WAVENC - Wake Vortex Evolution and Wake Vortex Encounter*. Publishable Synthesis Report, National Aerospace Lab., NLR-TR-2000-079, Amsterdam, The Netherlands, 2000.

[20] Fischenberg D. *Results of Flight Test Data Analysis*, SWAKE-TN-222_1, 2002.

[21] Jategaonkar R, Fischenberg D and Gruenhagen W. v. Aerodynamic Modeling and System Identification from Flight Data – Recent Applications at DLR, *Journal of Aircraft*, Vol. 41, No. 4, July – August 2004, pp 681-691, 2004.

[22] Schwarz C and Hahn K-U. Full-flight simulator study for wake vortex hazard area investigation, *AST – Aerospace Science and Technology*, 10 (2), Elsevier, pp 136-143, DOI 10.1016/j.ast.2005.09.005, March 2006.

[23] Fock H, Hahn K-U and Schwarz C. *Verwendung von vorausschauenden Strömungssensoren in Piloten-assistenzsystemen für den Wirbelschleppeneinflug* (Application of forward looking flow sensors for pilot assistance systems for wake vortex encounters), DLR report IB 111-2006/12, Braunschweig, Germany, 2006.

[24] Harris M, et al. Wake vortex detection and monitoring, *AST – Aerospace Science and Technology*, 6, Elsevier, 2002.

[25] Köpp F, et al. Characterization of Aircraft Wake Vortices by Multiple-Lidar Triangulation, *AIAA Journal,* Vol. 41, No. 6, June 2003.

[26] Rahm S, et al. Characterization of Aircraft Wake Vortices by Airborne Coherent Doppler Lidar, *Journal of Aircraft,* Vol. 44, No. 3, May – June 2007.

[27] Schmitt N P, Rehm T, Zeller P, Reithmeier G, Stilkerich S, Schertler H, Zinner H and Navé P. The AWIATOR Airborne LIDAR Turbulence Sensor. *Deutscher Luft- und Raumfahrtkongress 2005,* 2005-067, Friedrichshafen, Germany, 2005.

[28] Schwarz C and Hahn K-U. Safe Limits for Wake Vortex Penetration, *AIAA Atmospheric Flight Mechanics Conference*, Hilton Head Island, SC, 2007.

Copyright Statement

Figures

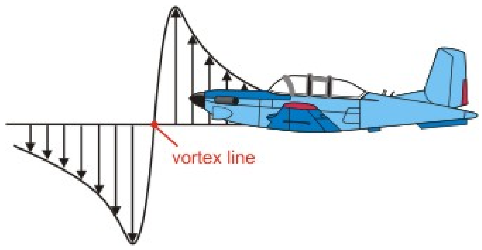

Fig. 1. Perpendicular wake vortex encounter

Fig. 2. DLC-flaps mounted on the ATTAS landing flap

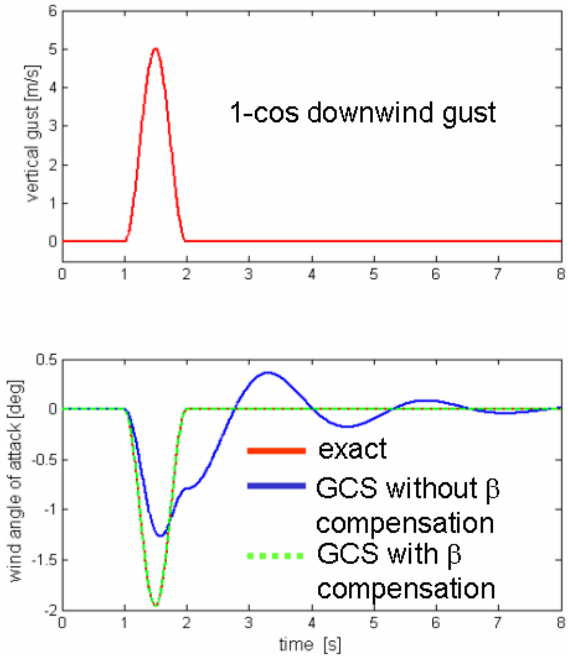

Fig. 3. Time histories of wind angle of attack

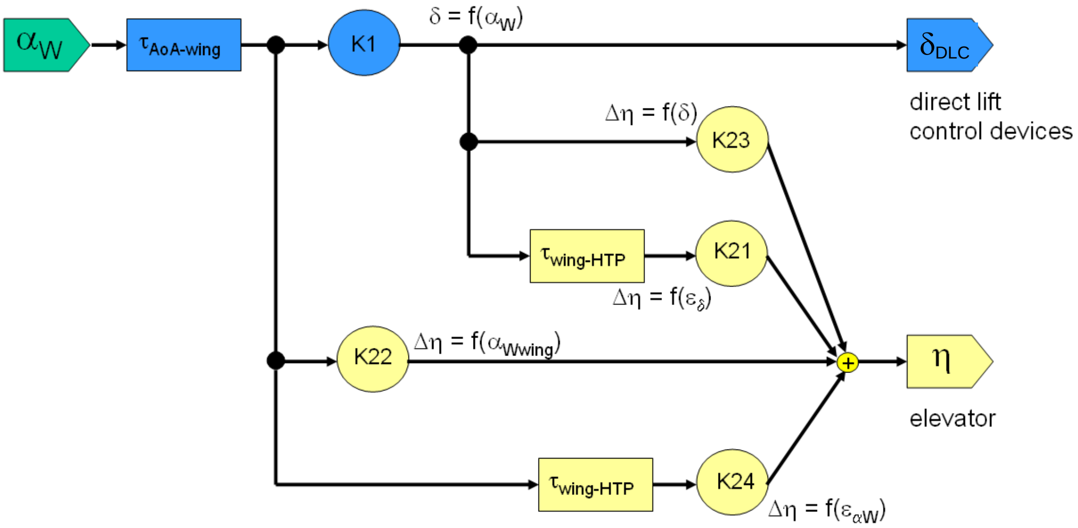

Fig. 4. Principle of normal acceleration and pitch compensation

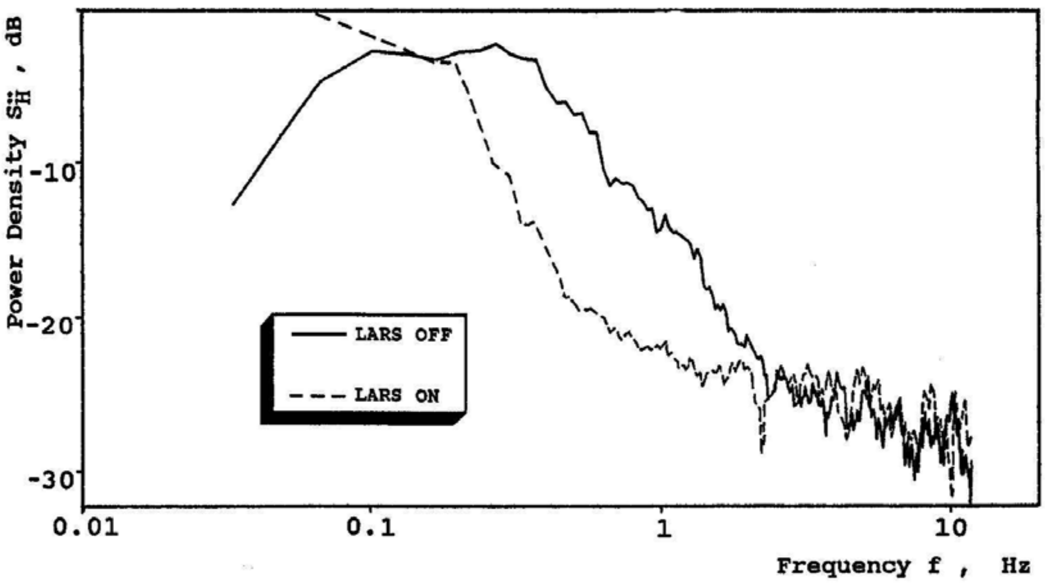

Fig. 5. Power density spectra of vertical load factor with and without LARS
(real flight test in homogeneous turbulence with a standard deviation of $\sigma_W \approx 0.35$m/s)

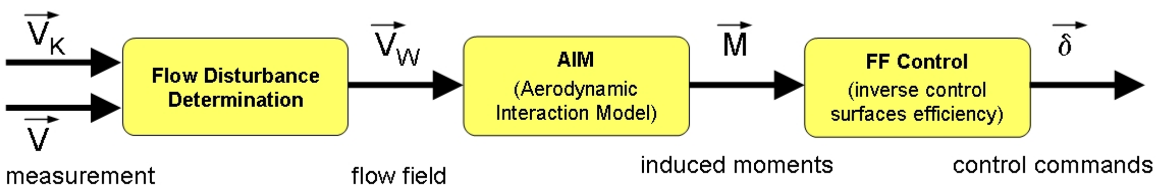

Fig. 6. Feed-forward wake vortex control concept

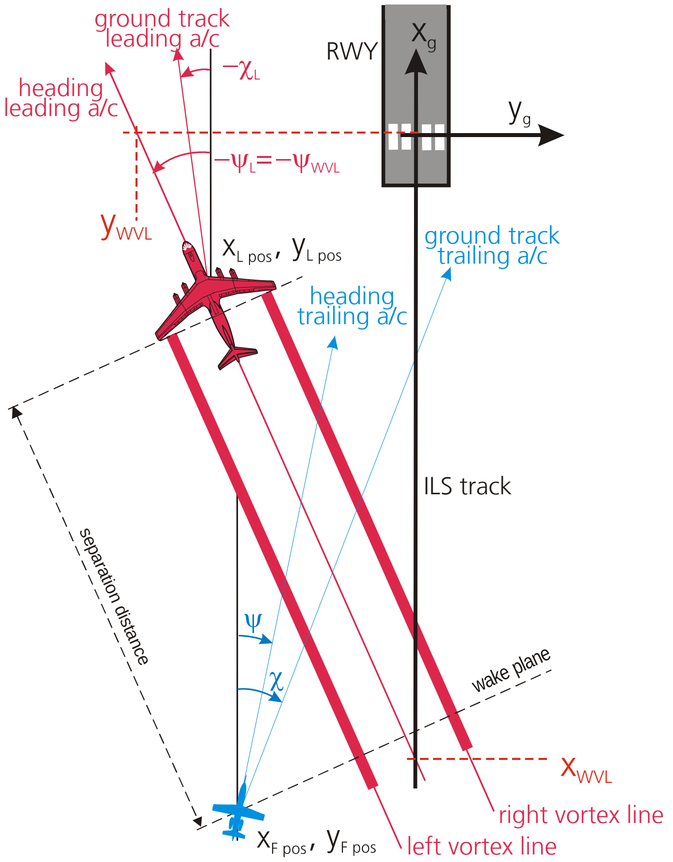

Fig. 7. Encounter scenario

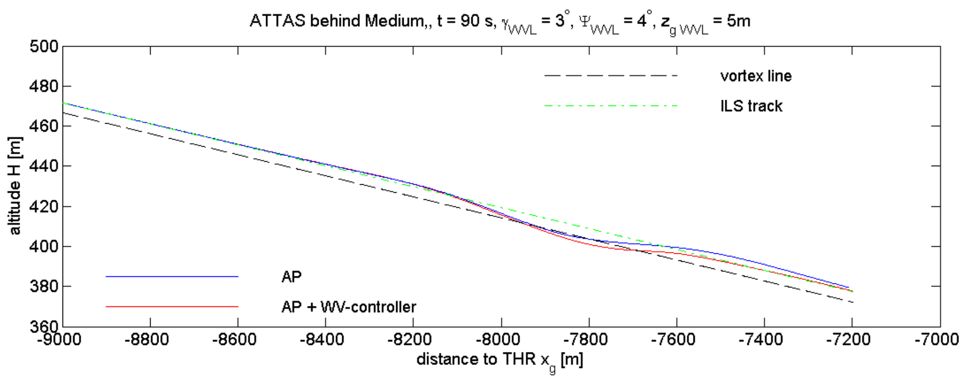

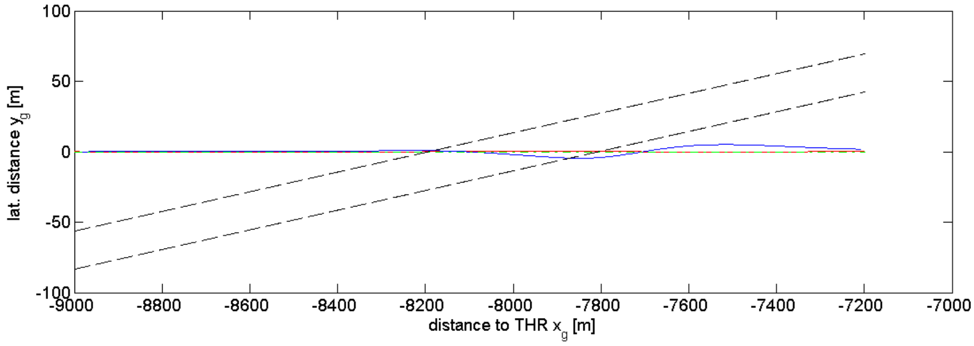

Fig. 8. Flight track of a flight through wake vortex flow field
(encounter angle: $\Delta\psi_{WVL} \approx 4°$, offline simulation with AP compared with combination AP plus wake vortex controller)

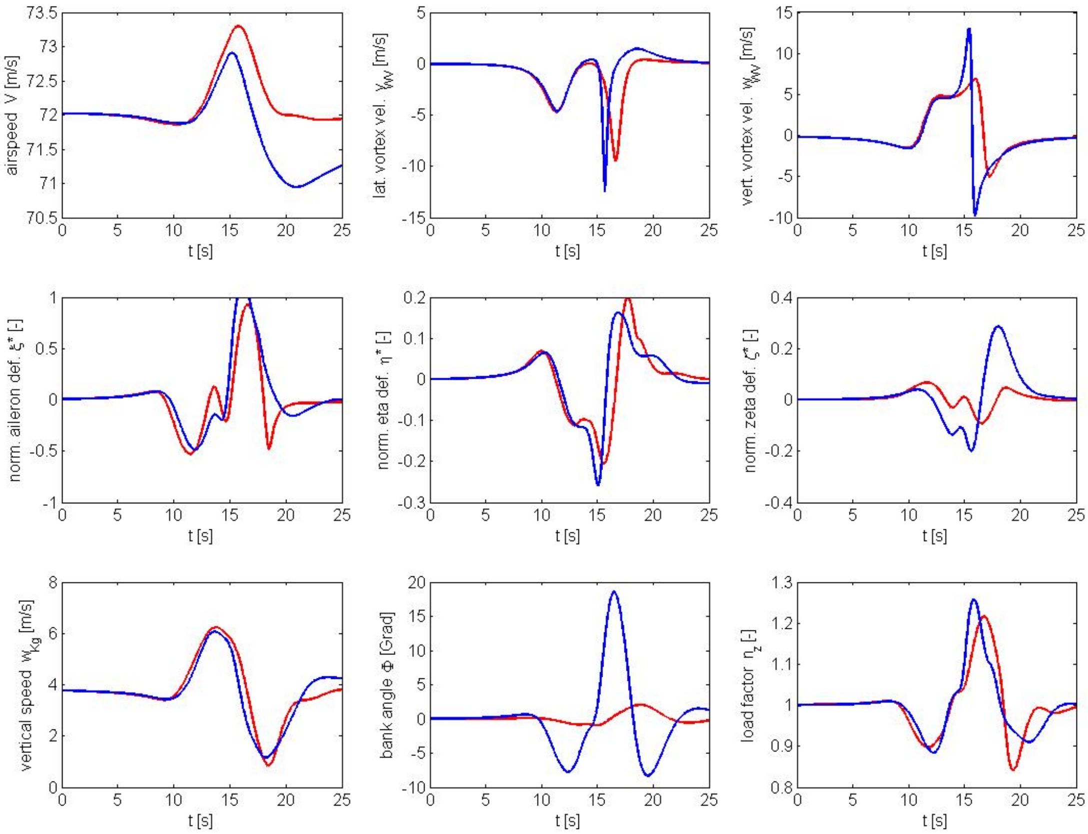

Fig. 9. Time histories of a flight through wake vortex flow field
encounter angle: $\Delta\psi_{WVL} \approx 4°$, offline simulation with AP [blue] compared with combination AP plus wake vortex controller [red]

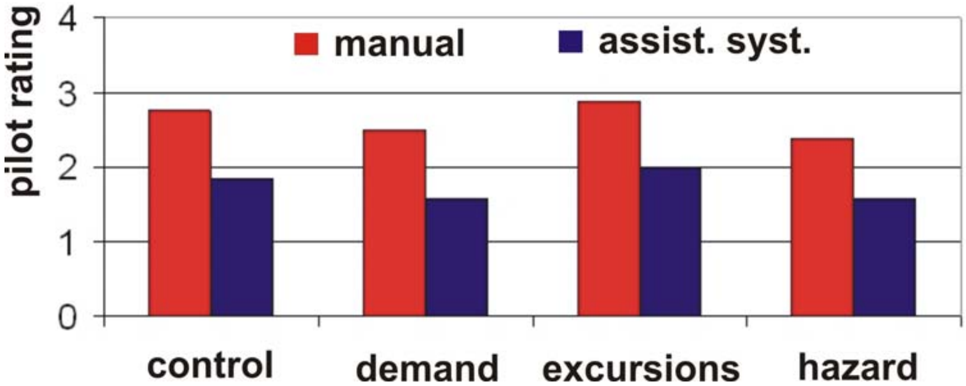

Fig. 10. Comparison of pilot ratings
(collected from flight tests)

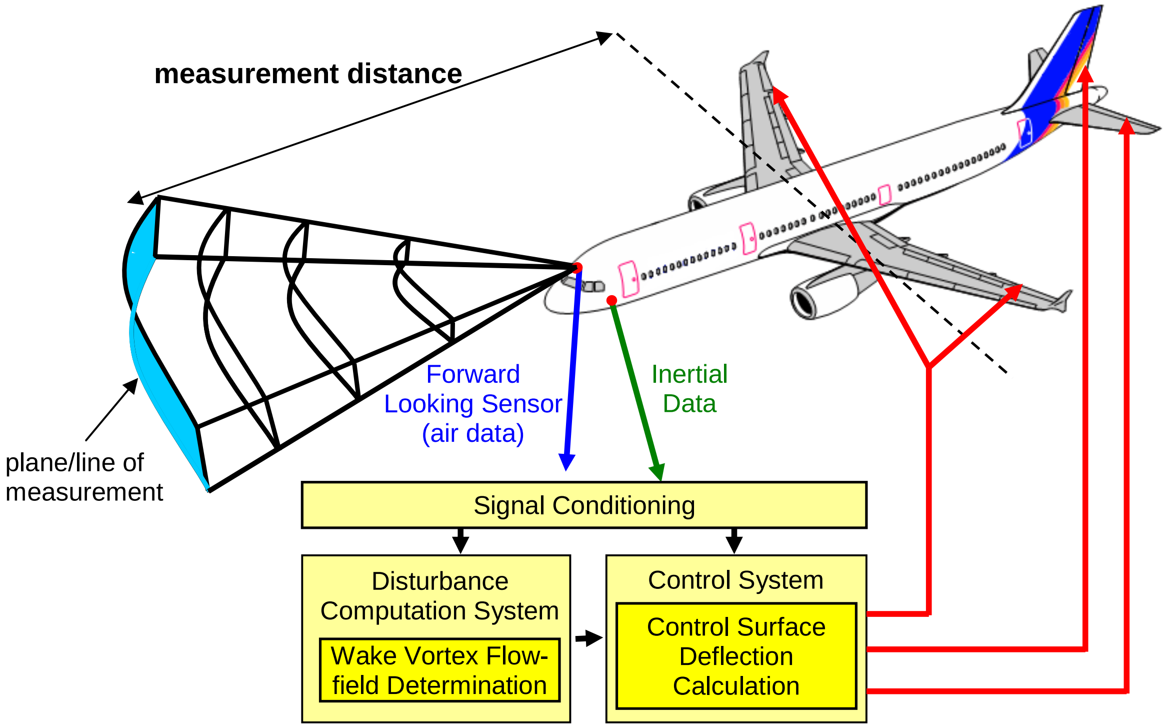

Fig. 11. Forward looking sensor concept

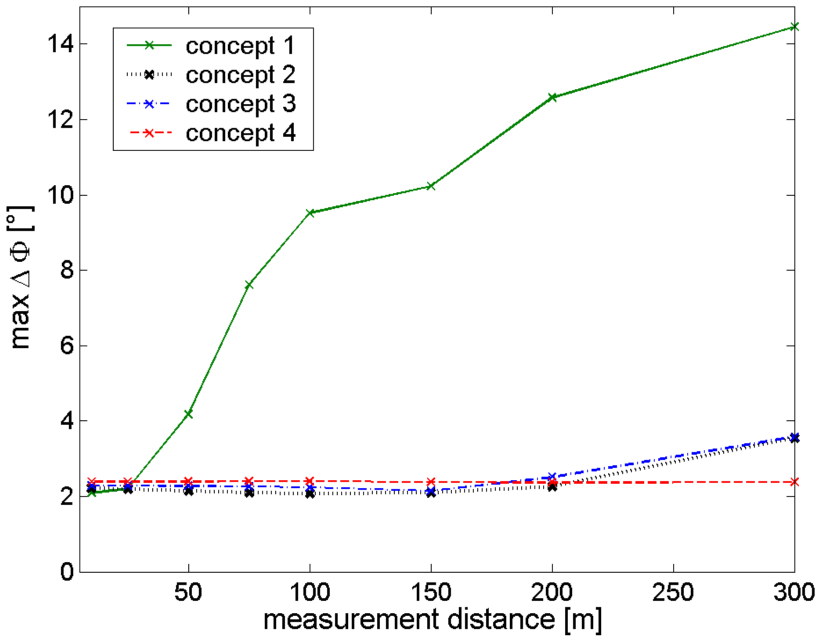

Fig. 12. Effect of applied concept and measurement distance on maximum bank angle

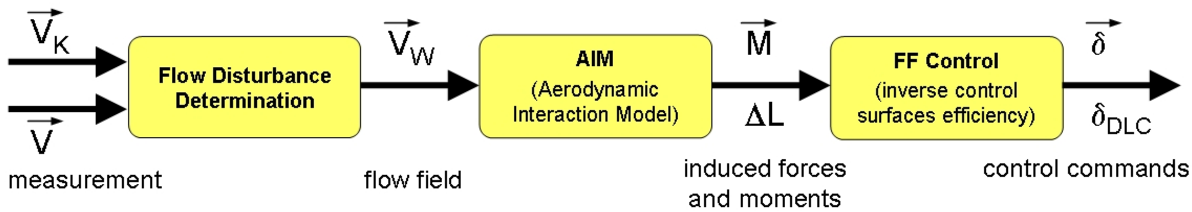

Fig. 13. Feed-forward wake vortex control and gust control concept

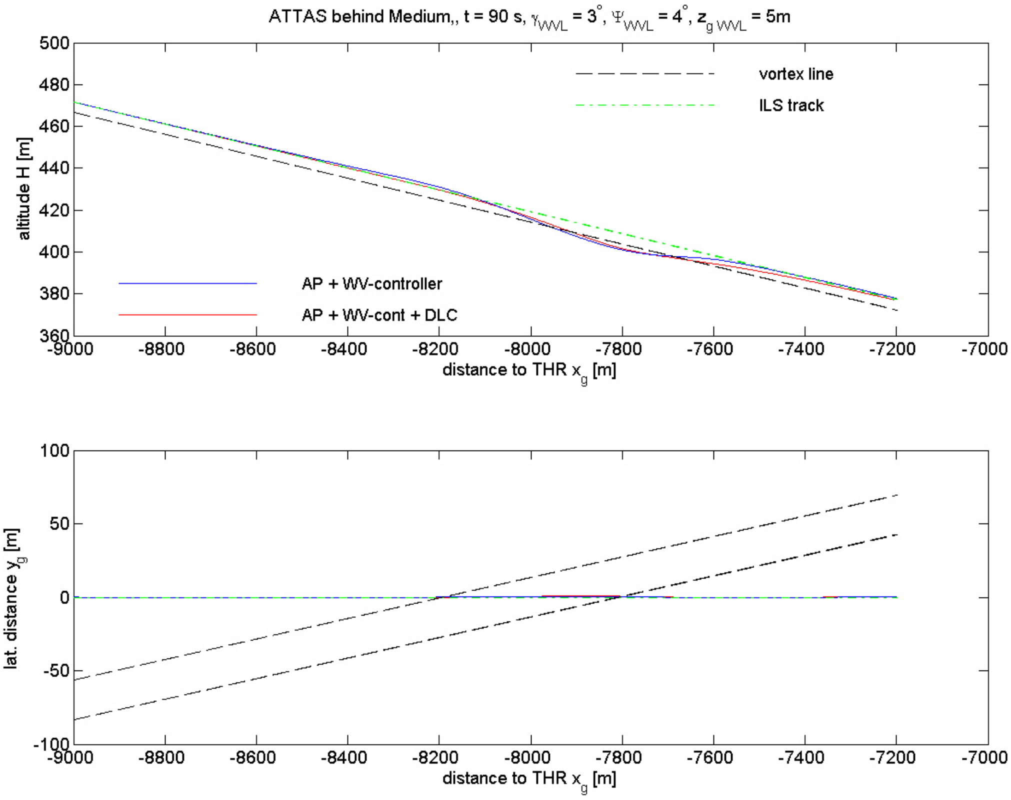

Fig. 14. Flight track of a flight through wake vortex flow field
encounter angle: $\Delta\psi_{WVL} \approx 4°$, offline simulation with combined AP plus wake vortex controller compared with IRLIS (combined AP plus wake vortex plus additional lift control)

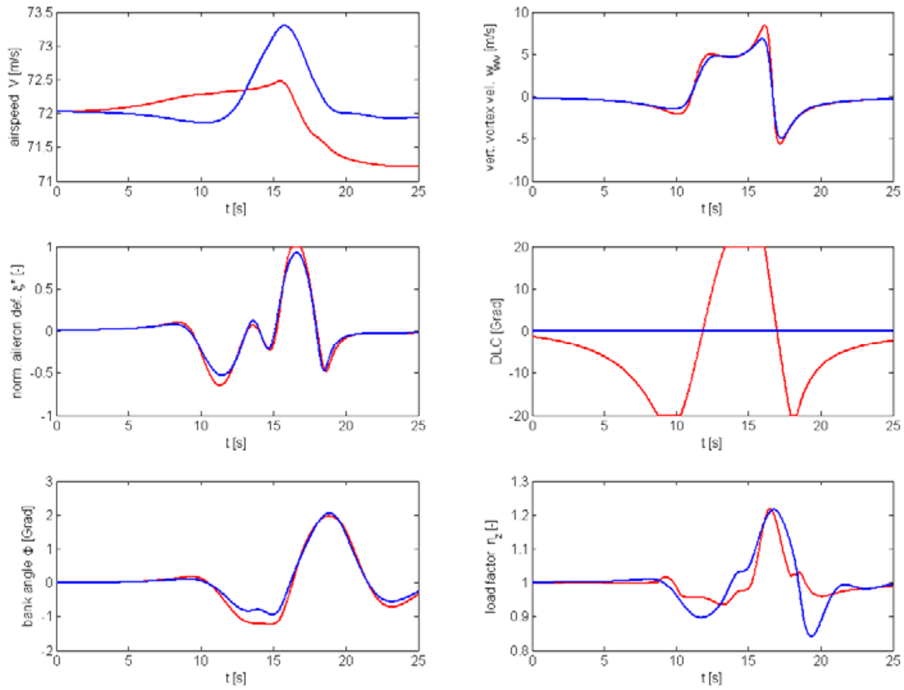

Fig. 15. Time histories of a flight through wake vortex flow field
encounter angle: $\Delta\psi_{WVL} \approx 4°$, offline simulation with combined AP plus wake vortex controller [blue] compared with IRLIS (combined AP plus wake vortex plus additional lift control [red])

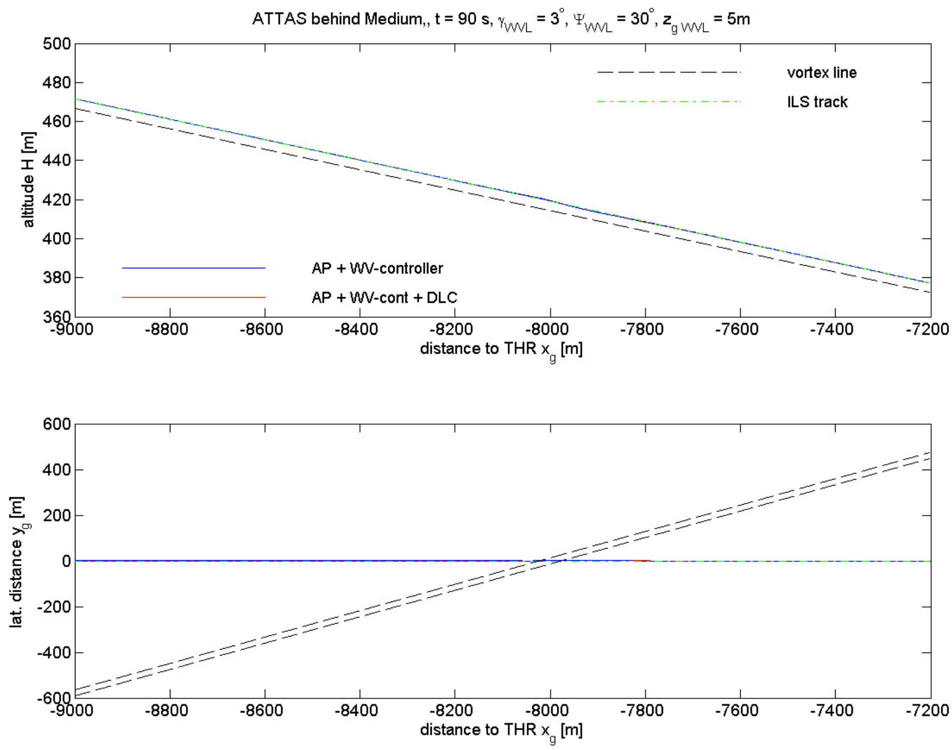

Fig. 16. Flight track of a flight through wake vortex flow field
encounter angle: $\Delta \psi_{WVL} \approx 30°$, offline simulation with combined AP plus wake vortex controller compared with IRLIS (combined AP plus wake vortex plus additional lift control)

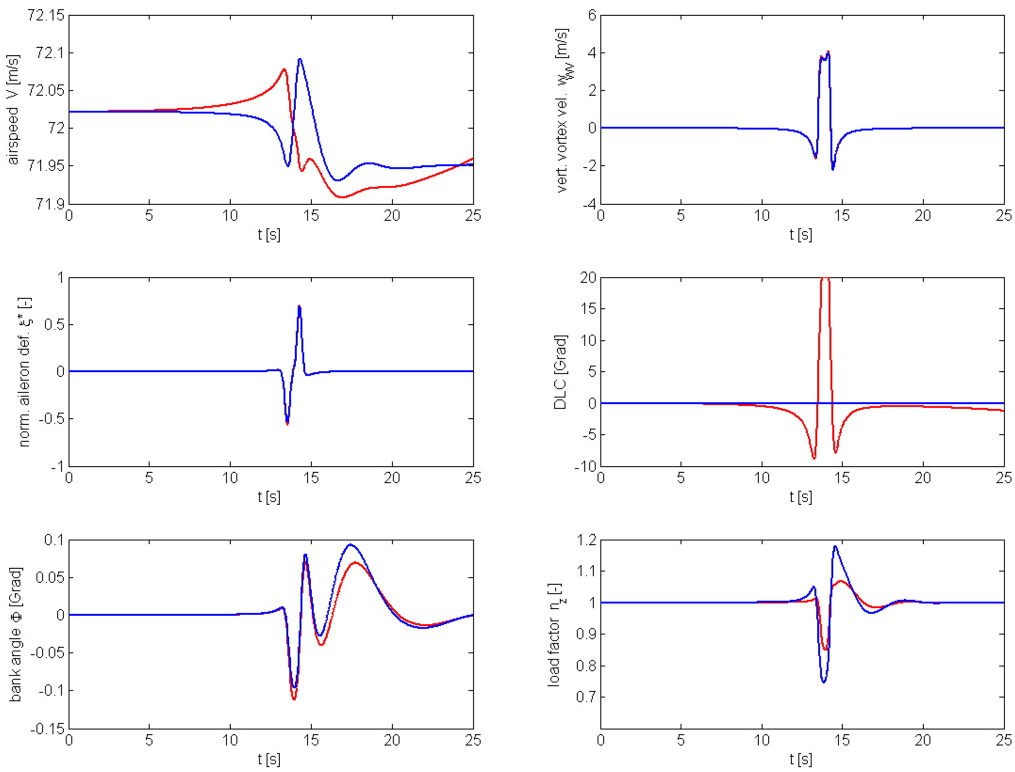

Fig. 17. Time histories of a flight through wake vortex flow field
encounter angle: $\Delta \psi_{WVL} \approx 30°$, offline simulation with combined AP plus wake vortex controller [blue] compared with IRLIS (combined AP plus wake vortex plus additional lift control [red])